Functional MRI of the Rodent Somatosensory Pathway Using Multislice Echo Planar Imaging

Shella D. Keilholz, Afonso C. Silva, Mira Raman, Hellmut Merkle, and Alan P. Koretsky*

A multislice EPI sequence was used to obtain functional MR images of the entire rat brain with BOLD contrast at 11.7 T. Ten to 11 slices covering the rat brain, with an in-plane resolution of 300 μm, provided enough sensitivity to detect activation in brain regions known to be involved in the somatosensory pathway during stimulation of the forelimbs. These regions were identified by warping a digitized rat brain atlas to each set of images. Data analysis was constrained to four major areas of the somatosensory pathway: primary and secondary somatosensory cortices, thalamus, and cerebellum. Incidence maps were generated. Electrical stimulation at 3 Hz led to significant activation in the primary sensory cortex in all rats. Activation in the secondary sensory cortex and cerebellum was observed in 70% of the studies, while thalamic activation was observed in 40%. The amplitude of activation was measured for each area, and average response time courses were calculated. Finally, the frequency dependence of the response to forepaw stimulation was measured in each of the activated areas. Optimal activation occurred in all areas at 3 Hz. These results demonstrate that whole-brain fMRI can be performed on rodents at 11.7 T to probe a well-defined neural network. Magn Reson Med 52: 89–99, 2004. Published 2004 Wiley-Liss, Inc.†

Key words: fMRI; BOLD; somatosensory stimulation; multislice

Functional MRI (fMRI) using blood oxygenation level-dependent (BOLD) contrast is a powerful technique for the noninvasive study of brain activation. In humans, BOLD contrast is widely used with multislice imaging sequences to study the activation of regions throughout the brain during a specific task (1–5). Animal models, particularly rodents, have played an important role in the early development of fMRI techniques (6–8), and in understanding the relation between neural activity and fMRI (9–14). While whole-brain fMRI studies are common in humans, they have been performed much less frequently in rodents. The small size of the rodent brain necessitates high resolution and complicates the acquisition of whole-brain functional images. Most of the BOLD fMRI studies performed in rodents have been limited to a few slices covering the sensory cortex in the rat. Much less work has been done in the mouse (9,15). Activation in the cortex during stimulation of the rat forepaw (13,14,16–18), hindlimb (16,19), tail (19), and whiskers (20) has been observed. Activation has also been observed in the olfactory bulb during presentation of odors (21,22). One study attempted to image the majority of the rat brain, but no activation was documented outside of the primary sensory cortex (23). The study was performed with an isotropic resolution of 1 mm, so it is likely that any activation in secondary areas was obscured by partial volume effects. Similarly, an fMRI study in a rat stroke model, using cerebral blood volume instead of BOLD, was performed at low resolution and observed only primary somatosensory cortex activation in the normal rats (24). Just one study has reported activation outside of the primary cortex, when activation was observed in the cerebellum during forepaw and hindpaw stimulation (25). This study only acquired data from the cerebellum.

Rodents have a well-characterized brain, ideal for the study of functional neural systems. Connections between many areas have been mapped by electrical recording and tract-tracing techniques. It is possible to perform behavioral studies in rodents, and surgical techniques have been used to manipulate neural systems. Thus, it is important to develop whole-brain fMRI in the rodent. The somatosensory pathway, in particular, is well described (26). A partial diagram is given in Fig. 1. Stimulation of the forepaw excites afferent nerves that travel through the spinal cord, synapse and cross the midline in the medulla, and are relayed to the ventroposterolateral nucleus (VPL) of the thalamus. Neurons from the thalamus project to layer 4 of the primary somatosensory cortex (SI) and also to the secondary somatosensory cortex (SII). These cortical areas project to the pons, where the information crosses the midline again and is relayed to the cerebellum. Given the degree of interconnectedness of the brain, this is only a partial description. There are reciprocal connections between most of the areas involved, as well as many connections to the contralateral hemisphere. The cerebellum also receives input directly from the spinal cord.

The robust activation of the primary sensory cortex detected by fMRI during electrical stimulation of the forepaw, along with the well-described connectivity of the rat somatosensory system, makes this an excellent model for development of robust whole-brain functional imaging in the rodent. Many studies have established that the rat SI activates during electrical stimulation of the limbs, but the expectations for other areas are not clear. Activation in SII has been widely reported in human sensory studies and should be detectable in rats as well. The thalamus must activate in order for the primary cortex to activate, but this is a small section in the rodent brain, making it difficult to detect with BOLD fMRI. By a similar argument, activation

Laboratory of Functional and Molecular Imaging, National Institutes of Neurological Disorders and Stroke, National Institutes of Health, Bethesda, Maryland.

Grant sponsor: NINDS intramural research program (Scientific Director Story Landis).

*Correspondence to: Alan P. Koretsky, Laboratory of Functional and Molecular Imaging, National Institute of Neurological Disorders and Stroke, NIH, 10 Center Dr., 10/B1D118, MSC 1065, Bethesda, MD 20892. E-mail: KoretskyA@ninds.nih.gov

Received 9 October 2003; revised 21 January 2004; accepted 8 February 2004.

DOI 10.1002/mrm.20114
Published online in Wiley InterScience (www.interscience.wiley.com).

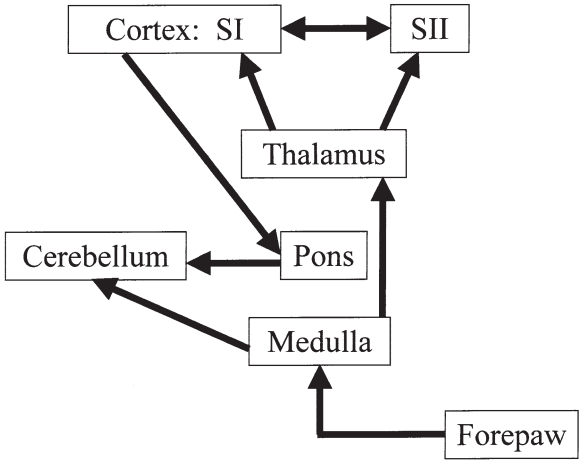

FIG. 1. Partial diagram of the somatosensory system. Impulses are conducted from the forepaw through the spinal column to synapse in the medulla. From there they are relayed to the thalamus and then to the sensory cortex. The cortex sends information to the pons, which relays it to the cerebellum. The cerebellum also receives input directly from the spinal cord.

should be present in the pons and medulla. Activation in the cerebellum has been reported in cerebellar studies of the rat during somatosensory stimulation, and so should be detectable in whole brain studies (25).

The requirements that whole-brain fMRI of small animals places on the imaging sequence and hardware are strenuous. Since many of the structures of interest are small (nuclei in the thalamus, pons, and medulla are ~300–800 μm across, and the areas of the nuclei involved in forepaw sensation are smaller still), high spatial resolution is essential, particularly in the coronal plane, but it is also necessary to keep the temporal resolution high enough to adequately sample the response to the stimulus without greatly lengthening the scans. The rat brain extends ~2.0–2.5 cm from the olfactory bulb to the cerebellum. To maximize coverage of the brain while maintaining temporal resolution, an echo planar imaging (EPI) sequence with interleaved slices was implemented on an 11.7 T, 31 cm horizontal bore MRI. The entire brain was imaged during a TR of 1.0–1.5 sec, at a spatial resolution of 300 × 300 × 2000 μm. This allowed the production of a functional map in 4 min. Robust activation was observed in the primary sensory cortex, secondary sensory cortex, and the cerebellum, with significant though less robust activation in the thalamus.

MATERIALS AND METHODS

Animal Preparation

All experiments were performed in compliance with guidelines set by the National Institutes of Neurological Disorders and Stroke ACUC. Eleven adult male Sprague-Dawley rats (168–234 g) were initially anesthetized with 5% halothane and maintained at 1.5% halothane during the following surgical procedures. Each rat was orally intubated and placed on a mechanical ventilator throughout the surgery and the experiment. Plastic catheters were inserted into the right femoral artery and vein to allow monitoring of arterial blood gases and administration of drugs. Two needle electrodes were inserted just under the skin of each forepaw, one between digits 1 and 2, and the other between digits 3 and 4. After surgery, the rat was given an i.v. bolus of α-chloralose (80 mg/kg) and halothane was discontinued. Anesthesia was maintained with a constant α-chloralose infusion (27 mg/kg/hr) (13).

The rat was placed on a heated water pad to maintain rectal temperature at ~37°C while in the magnet. Each animal was secured in a head holder with ear bars and a bite bar to prevent head motion and was strapped to a plastic cradle. End-tidal CO_2, rectal temperature, tidal pressure of ventilation, heart rate, and arterial blood pressure were continuously monitored during the experiment. Arterial blood gas levels were checked periodically and corrections were made by adjusting respiratory volume or administering sodium bicarbonate to maintain normal levels when required. An i.v. injection of pancuronium bromide (4 mg/kg) was given once per hour to prevent motion.

MRI

All images were acquired with an 11.7 T / 31 cm horizontal bore magnet (Magnex, Abingdon, UK), interfaced to an AVANCE console (Bruker, Billerica, MA) and equipped with a 9-cm gradient set, capable of providing 30 G/cm with a rise time of 65 μs. Shimming was performed with a custom-built shim set and high power shim supply (Resonance Research, Billerica, MA). A contoured rectangular surface coil (2 × 3 cm) that attached to the head holder was used to transmit and receive the MR signal. Scout images were acquired in three planes with a fast spin echo sequence to determine appropriate positioning for the functional study.

A spin-echo, EPI sequence was used for the fMRI studies. Setup included shimming, adjustments to echo spacing and symmetry, and B_0 compensation. A single-shot sequence with a 64 × 64 matrix was run with the following parameters: effective echo time 30 ms, repetition time 1.0–1.5 sec, bandwidth 200 kHz, field of view 1.92 × 1.92 cm. Whole-brain coverage was obtained with 10–11 2-mm thick slices, spaced 0.2 mm apart.

Somatosensory Stimulation Paradigm

A World Precision Instruments stimulator (WPI, Sarasota, FL) supplied 2 mA, 300 μs pulses repeated at 3 Hz to both forepaws upon demand. The paradigm consisted of 10 dummy scans to reach steady state, followed by 60 scans during rest, 30 scans during forepaw stimulation, and a final 60 scans during rest, for a total experiment time of 4 min. The animal was allowed to rest for ~3–5 min, and then the stimulation paradigm was repeated. To test the dependence of whole-brain activation on the stimulation frequency, stimulation was performed at 1 Hz, 3 Hz, 5 Hz, and 8 Hz in four rats.

Data Analysis

Analysis of the time series was performed using STIMULATE (University of Minnesota, Minneapolis,

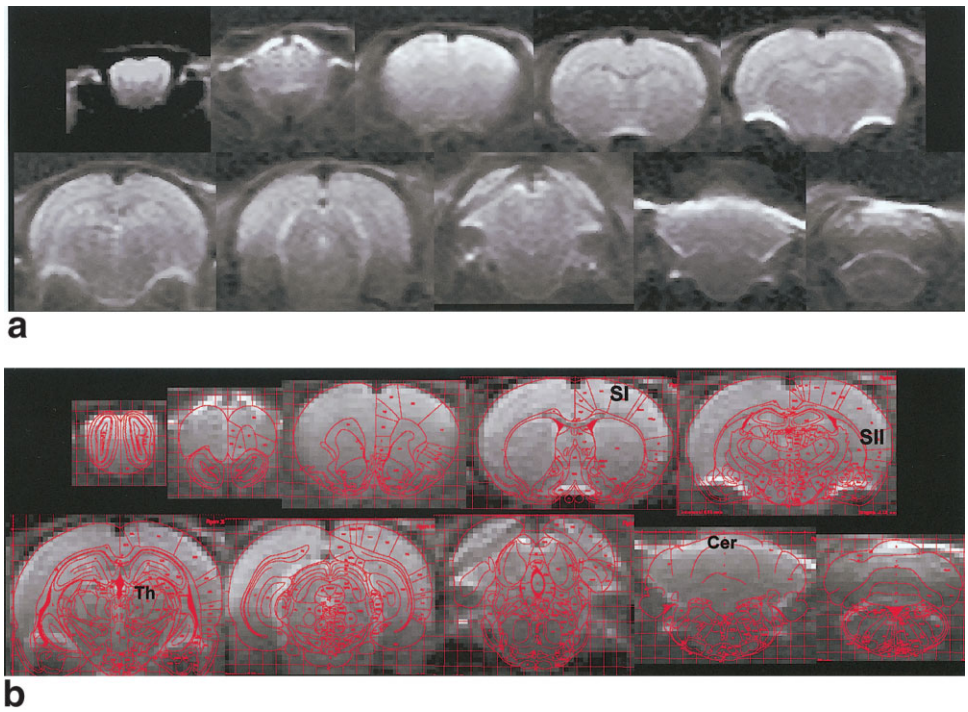

FIG. 2. **a:** Typical EPI images with in-plane resolution of 300 μm and 2 mm slice thickness. Ten slices cover the brain from the olfactory bulb (top left) to the cerebellum (bottom right). **b:** EPI images from the same rat overlaid with the digitized rat brain atlas. A linear warp in x and y was performed on each atlas image to provide the best fit to the corresponding EPI slice. The locations of SI, SII, thalamus (Th), and cerebellum (Cer) are indicated.

MN). A correlation coefficient was calculated from cross-correlation of the unfiltered time series with a boxcar waveform representing the stimulation period. The activation threshold was set at 0.2, and only groups that included at least four activated pixels were considered significant. One to three scans from each animal were analyzed, depending on the stability of the animal and whether blood gases remained within physiological ranges. Time courses from activated pixels in SI, SII, thalamus, and cerebellum were recorded and averaged to form a representative response for each region. A linear baseline correction was performed.

Using a customized program developed in-house, the Paxinos and Watson rat brain atlas (27) was digitized so it could be warped to each MRI slice containing a specific region of interest (ROI). The location of the activated pixels of that slice in relation to the atlas could be saved. The same program was then used to read in the atlas images with activated pixels from each rat and add them together to display the relative incidence of activation in each region in the atlas coordinate system.

For the frequency dependence studies, the number of activated pixels in SI, SII, the thalamus, and the cerebellum was recorded for each rat and average activation areas were obtained for each frequency of stimulation. Using the rat brain atlas, areas were then defined in SI, SII, and the cerebellum, and time courses from all the pixels in the region were obtained from each rat. These were averaged to show the amplitude of the BOLD response in each area as a function of frequency. Statistical significance was calculated using a paired *t*-test. Unless otherwise noted, differences were considered significant at $P < 0.05$.

RESULTS

Stability of the Imaging Sequence

Typical whole-brain EPI images of the rat obtained at 11.7 T are shown in Fig. 2a. The cerebral cortex and cerebellum are well visualized, but there is clearly some distortion near the sinuses. Figure 2b shows a set of EPI images from the same rat with the Paxinos atlas warped to each slice, using only linear warps in the horizontal and vertical directions (27). Despite the single-shot EPI acquisition at 11.7 T, the atlas fits very well to the images. SI, SII, thalamus and cerebellum are labeled.

In order to demonstrate the temporal stability of the multislice imaging sequence, a series of 150 images was acquired from an anesthetized rat without the application of a stimulus. The signal intensity of each image was measured in ROIs in SI, SII, thalamus, and cerebellum. The percent deviation from the mean signal intensity in each region was calculated for the series of images and is shown in Fig. 3. The stability was very good, generally exhibiting about ±1% fluctuation around the average intensity in each region, even though no respiratory or cardiac gating was used. This allows ready detection of the BOLD response, where the intensity change is on the order of 5–10% at 11.7 T (14).

Incidence and Amplitude of Activation

Twenty-four functional studies were obtained from 11 rats. In the correlation maps calculated with STIMULATE, activation was repeatedly seen in four areas: SI, SII, thalamus, and cerebellum. Small clusters of pixels with low correlation coefficients were observed in other areas as well, but they were not reproducible and thus were not

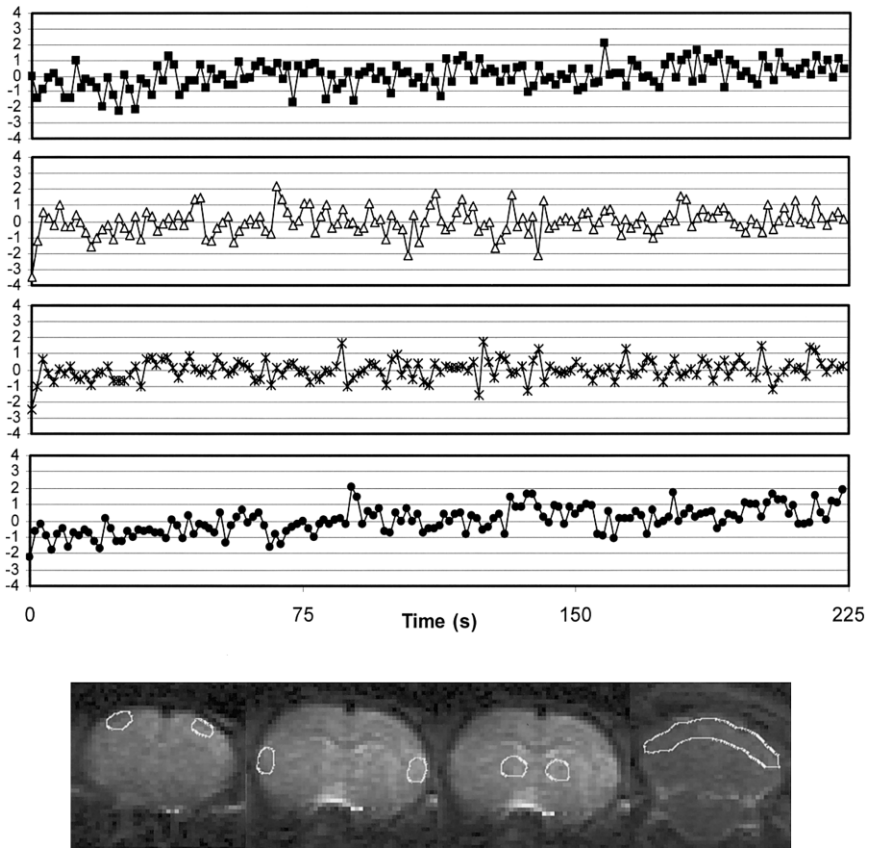

FIG. 3. Temporal stability of EPI images acquired in an anesthetized rat. The percent fluctuation from the mean as measured in (from top to bottom) SI, SII, thalamus, and cerebellum during a series of images acquired with no stimulation is shown. No baseline correction has been performed. The ROIs in which the signal was measured are shown in white on the EPI images below.

included in the analysis. Typical fMRI results from two rats are shown in Fig. 4.

The primary cortex showed significant activation in all rats and all studies, with an average peak signal intensity increase of 7.5% ± 1.8% (11 rats, 24 scans). Given that the forelimb representation in SI is elongated 3–4 mm in the rostral–caudal direction, activation often extended to at least one and often two adjacent slices. Our results were similar to those seen in previous work (12–14,16,17).

The cerebellum also responded robustly, showing activation in 8/11 rats. The activated areas formed a patchy cluster near the superior surface of the cerebellum, often

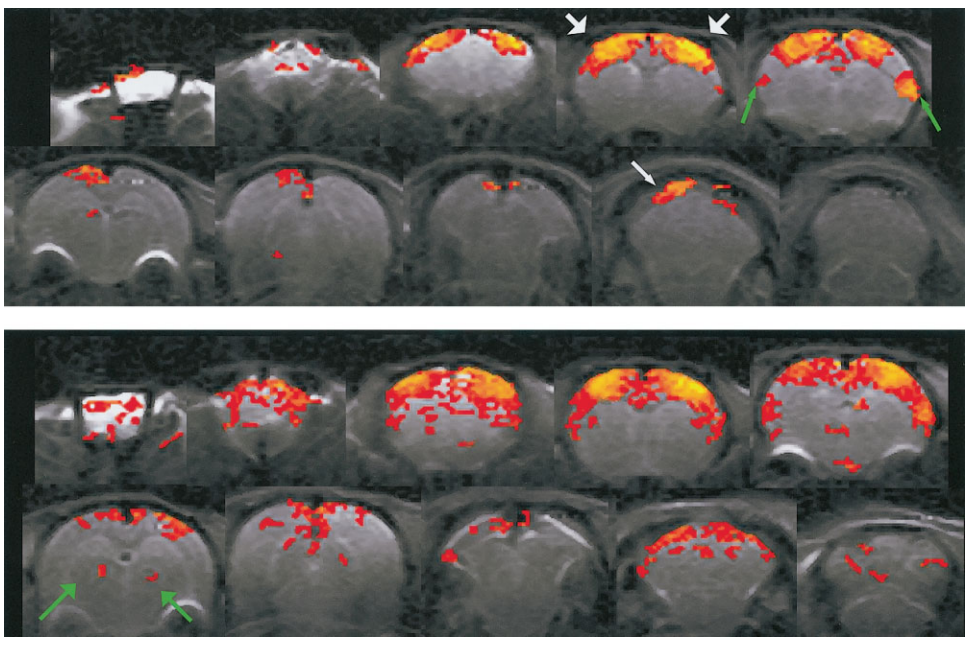

FIG. 4. Typical findings in whole-brain functional images during forepaw stimulation. The correlation threshold was set at 0.2, and groups of 4 or more active pixels are shown. Slices progress from most anterior at top left to most posterior at bottom right. Top: activation in SI (large white arrows), SII (green arrows), and the cerebellum (small white arrow). Bottom: activation in SI, SII, the cerebellum, and the thalamus (large green arrows).

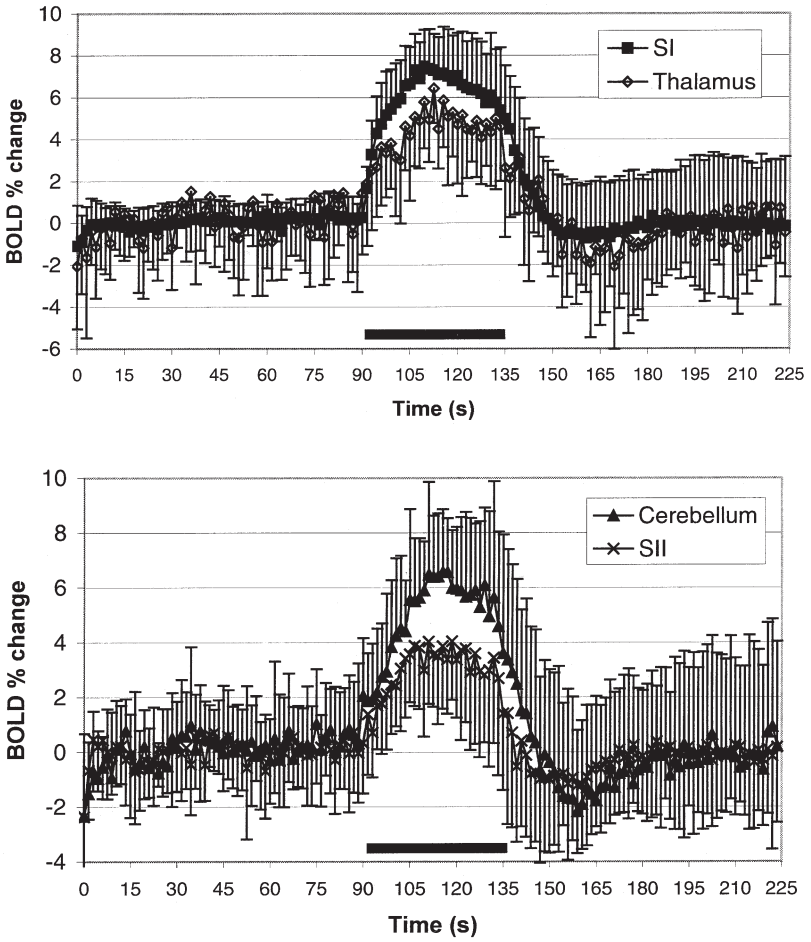

FIG. 5. Average time courses measured from the activated regions of the primary cortex and thalamus (top) and secondary cortex and cerebellum (bottom). The average increase in SI was significantly greater than the increase in SII, thalamus, or cerebellum ($P < 0.005$). The duration of the stimulus is indicated by the black bar. Error bars = 1 SD.

with bilateral focus areas. These results agree well with a previous study (25). The amplitude of the response is lower than that of the primary cortex, with an average peak increase of 6.6 ± 1.9% (8 rats, 16 scans).

Activation was observed in SII in 8/11 rats, although the magnitude of the signal intensity increase during stimulation was smaller than in the primary cortex and cerebellum, averaging 4.0% ± 1.8% (8 rats, 18 scans). The activated areas were inferior and lateral to the primary sensory cortex, and located either in the same image slice as SI or the slice immediately posterior.

Activation was also observed in the thalamus in one or two slices immediately posterior to SI, but only in 5/11 rats. It was generally detected only when strong activation was present in at least two other areas. The average peak signal increase when activation was observed was 6.4 ± 1.9% (five rats, nine scans).

Average time courses from each area are shown in Fig. 5. In general, the BOLD signal from each area reached a peak within ~15 sec after the beginning of the stimulation, remained at a plateau for the rest of the stimulation, and returned to baseline ~15 sec after the stimulation ended. Some areas show a temporary decrease below baseline values for several seconds after the end of the stimulation. The average increase in signal intensity in SI was significantly greater than the increase in SII, thalamus, or cerebellum ($P < 0.005$). The most pronounced differences in response between areas were the amplitude of the BOLD signal and the magnitude of the poststimulus undershoot. Only a very small undershoot is evident in the time course from SI; SII and the thalamus show moderate undershoots, while the cerebellum has a significant decrease in intensity of 2% that requires ~30 sec to return to baseline levels.

Figure 6 summarizes the incidence of activation across the rats studied. The images show the variation in area of the responses detected for SI, SII, thalamus, and cerebellum. SI was detected in all rats. Cerebellum and SII activated in 67% and 75% of the rats. The thalamus was the least consistent, activating in only about 40% of the rats.

Activation incidence maps were generated by transferring areas of activation to the Paxinos atlas, so that each activation could be mapped to a common space (27). Figure 7 shows incidence maps for SI, SII, thalamus, and cerebellum. Excellent inter-rat correspondence of activated areas leads to bright focal points in SI, SII, and the cerebellum. Thalamus can also be seen, although it activated in fewer rats.

Frequency Dependence

The frequency dependence of blood flow changes and fMRI response has been studied in SI by a number of

	Total Scans	Total Rats
SI	24 (100%)	11 (100%)
Cerebellum	16 (67%)	8 (73%)
Thalamus	9 (38%)	5 (45%)
SII	18 (75%)	8 (73%)
SII + Thalamus	5 (21%)	3 (27%)
SII + Cerebellum	11 (46%)	6 (55%)
Cerebellum + Thalamus	7 (29%)	3 (27%)
SII + Cerebellum + Thalamus	4 (17%)	2 (18%)

a

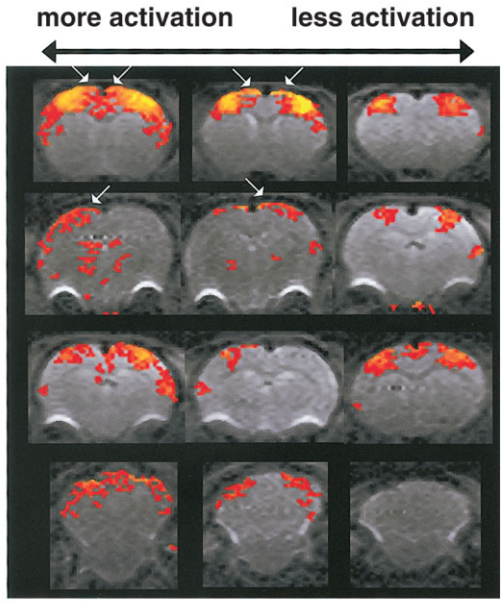

b

FIG. 6. Summary of activation incidence. A total of 24 scans were obtained in 11 rats. **a:** The incidence of activation for each area and combination of areas. **b:** Representative images from different rats demonstrating the variance in activation in SI, thalamus, SII, and cerebellum are shown. Arrows indicate regions of activation that likely arise from draining veins.

investigators using the rat forepaw model (13,28–31). To extend this to other areas of the brain, data was acquired at different stimulation frequencies. Typical activation maps acquired during stimulation at 1 Hz, 3 Hz, 5 Hz, and 8 Hz are shown in Fig. 8. The largest activation in SI, SII, and the cerebellum is seen at 3 Hz, with less activity at 5 Hz. Average numbers of pixels activated for each frequency are shown in Fig. 9. Average time courses from each area are shown in Fig. 10. In SI, the percent signal change during activation is greatest for 3 Hz, followed by 5, 8, and 1 Hz. The percent change was also strongest at 3 Hz in SII, with no large differences between 1, 5, and 8 Hz. The cerebellum also exhibited the strongest activation at 3 Hz. Only one rat showed cerebellar activation at 8 Hz. No time courses were measured for the thalamus due to the intermittent nature of the activation. These frequency-dependent results are similar to those described in previous studies of the primary somatosensory cortex, which generally have found peak response at stimulation frequencies of 3–5 Hz (13,28,29).

DISCUSSION

The excellent EPI images obtained in this study can be attributed to several factors, including the high field strength, the use of a surface receive coil, an optimized imaging sequence, the high-power shims, and the rapidly switching gradient set. Working at 11.7 T provides excellent signal-to-noise and a larger BOLD effect. The use of the surface coil restricts the field of view and provides optimal sensitivity to the ROIs. The shims and the gradients are especially important in reducing distortion in the image.

The results presented clearly demonstrate that whole-brain fMRI can be performed in rodents using EPI at 11.7 T. Activation was observed in four of the six regions involved in primary sensory pathways: SI, SII, thalamus, and cerebellum. No activation was detected in the pons or medulla, most likely due to the deep location of these structures and the signal sensitivity falloff from the surface coil. Future studies that begin to make use of surface coil arrays should remedy the problem.

The number of activated regions differed from rat to rat. SI activated consistently in every scan and always had a greater signal increase during stimulation than the other activated areas. A slight discrepancy in incidence ($n = 2–3$ scans) between the left and right hemispheres was seen. Since no special care was taken to ensure that the stimulators to each paw were supplying exactly the same current, stimulation disparities could easily account for the minor difference. The activated area of SI spreads beyond the boundaries indicated on the rat brain atlas. However, the pixels with the highest correlation coefficients and largest incidence generally lie within the area defined by the atlas. Raising the threshold correlation coefficient to levels typically used in other studies (12–14) results in better localization but reduces sensitivity to secondary areas with lower signal increases, such as SII.

SII and the cerebellum each activated in about 70% of the scans, and activation in both occurred in 50% of the scans. Thalamic activation was observed less frequently, and usually only in conjunction with activation in SII or the cerebellum. There are several potential explanations for why activation may be seen in a given area in one rat but not in another. One possibility is the effect of partial volume on small active regions. If an active area is approximately the size of a voxel ($300 \times 300 \times 2000$ μm), then the activation is more likely to be seen if the area falls within a single voxel, rather than being divided between two or three. The alignment between image geometry and anatomy differs in each rat, and may in some cases cause

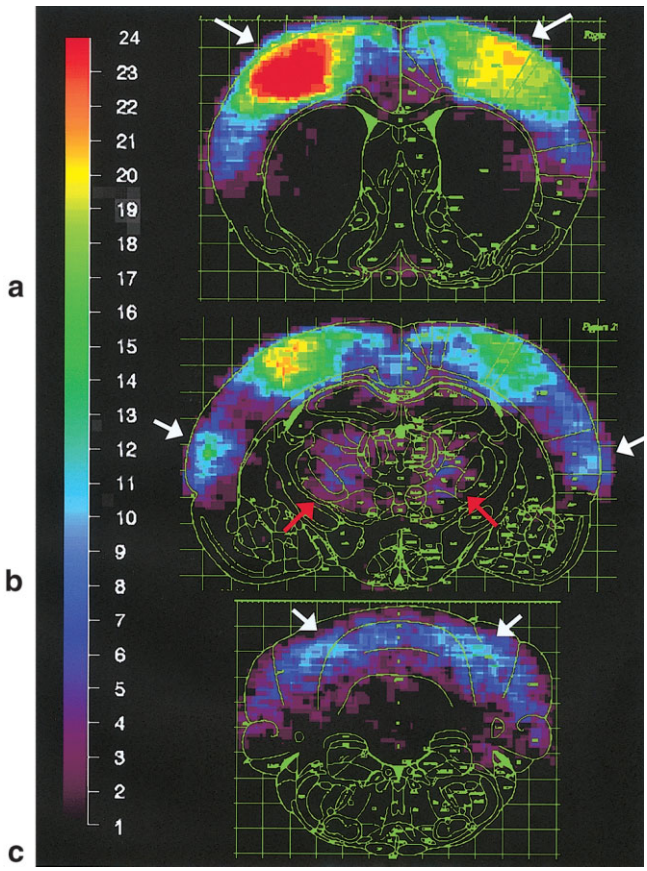

FIG. 7. Activation maps from individual rats overlaid onto the Paxinos atlas and summed to show incidence of activation. Distinct areas in SI (arrows, **a**), SII (white arrows, **b**) and the thalamus (red arrows, **b**) are apparent, along with bilateral focal regions in the cerebellum (arrows, **c**). Incidence ranges from 1 to 24 scans.

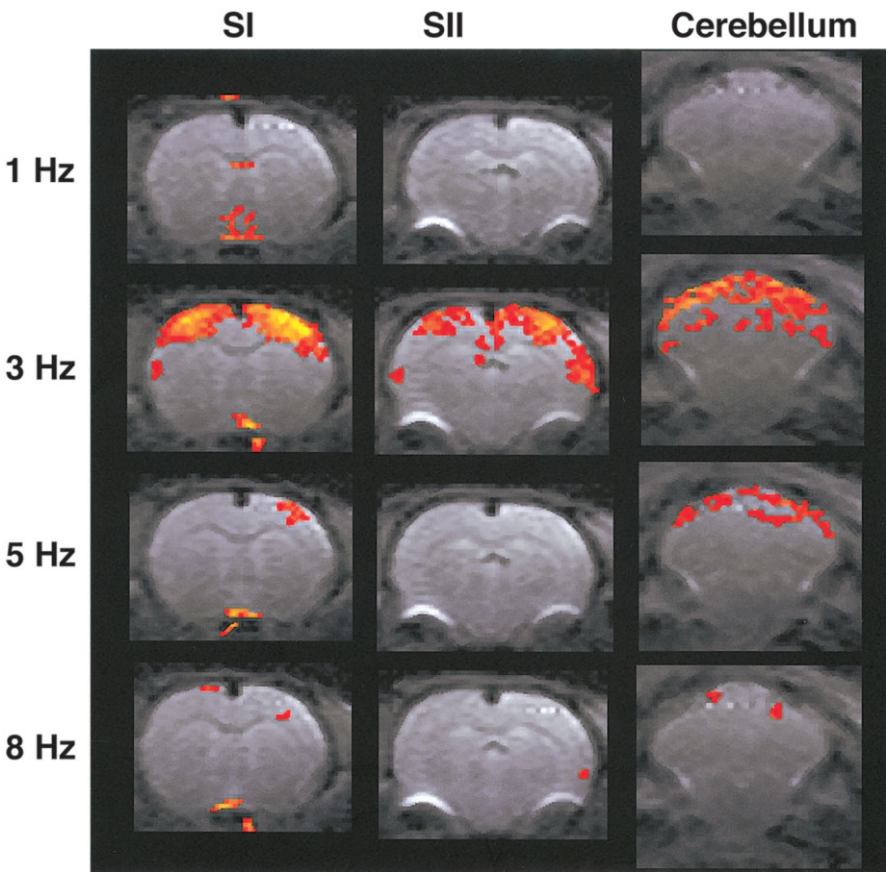

FIG. 8. Response to 1, 3, 5, and 8 Hz stimulation in slices from SI, SII, and cerebellum. The largest activated area occurs at 3 Hz for all areas.

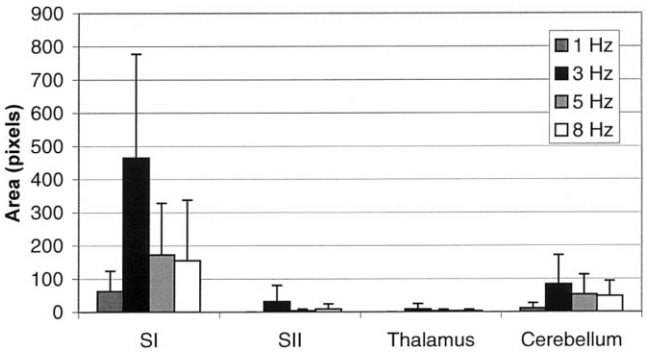

FIG. 9. Area of activation in SI, SII, cerebellum, and thalamus measured for different stimulus frequencies.

reduction in the observed BOLD response or render small regions of activation undetectable. Also, while regions in the somatosensory system generally range in size from 300 μm to 2 mm, only a fraction of each area is specifically devoted to forelimb sensation, which exacerbates the sensitivity loss due to partial volume effects. Future studies should enable us to improve resolution.

An issue which affects the SNR of the image and thus the probability of detecting the BOLD response is the location of the region with respect to the surface coil. SII and the thalamus are located further from the surface coil than SI and the cerebellum, and in large rats the loss of signal sensitivity (20–40% lower SNR) may make it difficult to observe activation. Development of surface coil arrays analogous to that occurring for the human brain should improve sensitivity in these regions as well as enable acceleration of image acquisition using parallel imaging techniques (32,33).

A major concern for rodent fMRI is the use of anesthesia. It is possible that the degree of activation depends on the animal's level of awareness. A previous study has shown that α-chloralose reduces the area of activation and depresses the amplitude of the BOLD signal increase in SI during stimulation of the forepaw (34). Thus, an explanation for the lack of consistent thalamic activation may be that it is detected only in animals that are less deeply anesthetized. The ability to compare whole-brain fMRI in awake and anesthetized rodents will enable investigation of this issue for all areas in a specific neural network (35,36).

There has been much interest in fMRI in the details of the time course of the hemodynamic response. Issues include the existence of an initial dip in the BOLD signal just before the rise that occurs during stimulation and the origins of the poststimulus undershoot (37). The present study shows no significant initial drop in signal, in agreement with previous results (14,38). The average time courses measured in this study show a significantly greater signal undershoot in SII, the thalamus, and the cerebellum than in SI after the stimulation period. This may indicate regional differences in hemodynamics, perfusion, or metabolism. For example, the increase in cerebral blood volume during stimulation may take longer to return to baseline in areas other than SI.

Numerous issues exist regarding the quantitative connection between BOLD fMRI and the complex underlying neural activity (12,39,40). A major issue is the relative contribution of different size vessels. Some of the activation observed in this experiment clearly comes from large draining veins. Activation from veins draining from SI along the surface to the center of the brain could be detected in many rats (see Fig. 6b), even though spin echo BOLD was used at 11.7 T. The BOLD signal is made up of contributions from the intravascular and extravascular compartments of small and large veins. The extravascular signal from small vessels is generally considered to be the most localized to neuronal activity, but it can easily be obscured by the large signal from inside veins and the extravascular area around large draining veins. Simulations and some experiments have indicated that, compared to gradient-echo imaging, spin-echo imaging reduces the contribution of the extravascular compartment of large vessels, due to the smaller susceptibility gradients and the refocusing effect of the 180° pulse (39,40). In addition, the same studies have argued that the intravascular contributions to the BOLD signal, as measured with a spin-echo sequence, are expected to be very small at high field strengths, due to the short T_2 and T_2^* of venous blood. In favor of this latter argument, a recent study by Lee et al. (12) demonstrated that there was no change in the spin-echo BOLD signal obtained at 9.4 T when diffusion gradients were applied, suggesting that the intravascular contribution is negligible. In some of the images acquired in this experiment, a thin line of activation appears to stretch from SI toward the sagittal sinus along the surface of the brain (Fig. 6b), similar to activation attributed to draining veins in previous work (12–14). This signal may arise from incomplete suppression of the extravascular signal associated with large veins, or from residual intravascular contributions. While spin-echo EPI was used to acquire the data, the images have significant T_2^* weighting from the gradient echoes in the EPI readout. Also, although the signal inside the veins is small, the change in R_2 during activation is large, and may lead to a strong correlation with the stimulus.

Previous studies of changes in cerebral blood flow during stimulation have indicated that there is a stimulation frequency to which SI is maximally responsive (13,28–31). Activation is expected to increase as the frequency of stimulation increases, since there are more stimuli per unit time. At some point, however, as the interval between stimuli shortens, the second stimulus occurs during the refractory period caused by the first stimulus, and activation decreases. Gyngell et al.(30) tested 1.5, 3, 4.5, 6, 7.5, and 9 Hz and found the greatest change in BOLD at 1.5 Hz. Using laser Doppler, Detre et al. (29) tested 1, 2, 5, and 10 Hz and observed a maximum blood flow change at 5 Hz. A similar study by Silva et al. (13) tested 1, 2, 3, 4, and 5 Hz and saw the greatest change in blood flow at 3 Hz. All of these studies focused on the primary sensory cortex, and it was unknown whether the secondary sensory cortex and cerebellum would follow the same pattern. The present results are consistent with these previous studies,

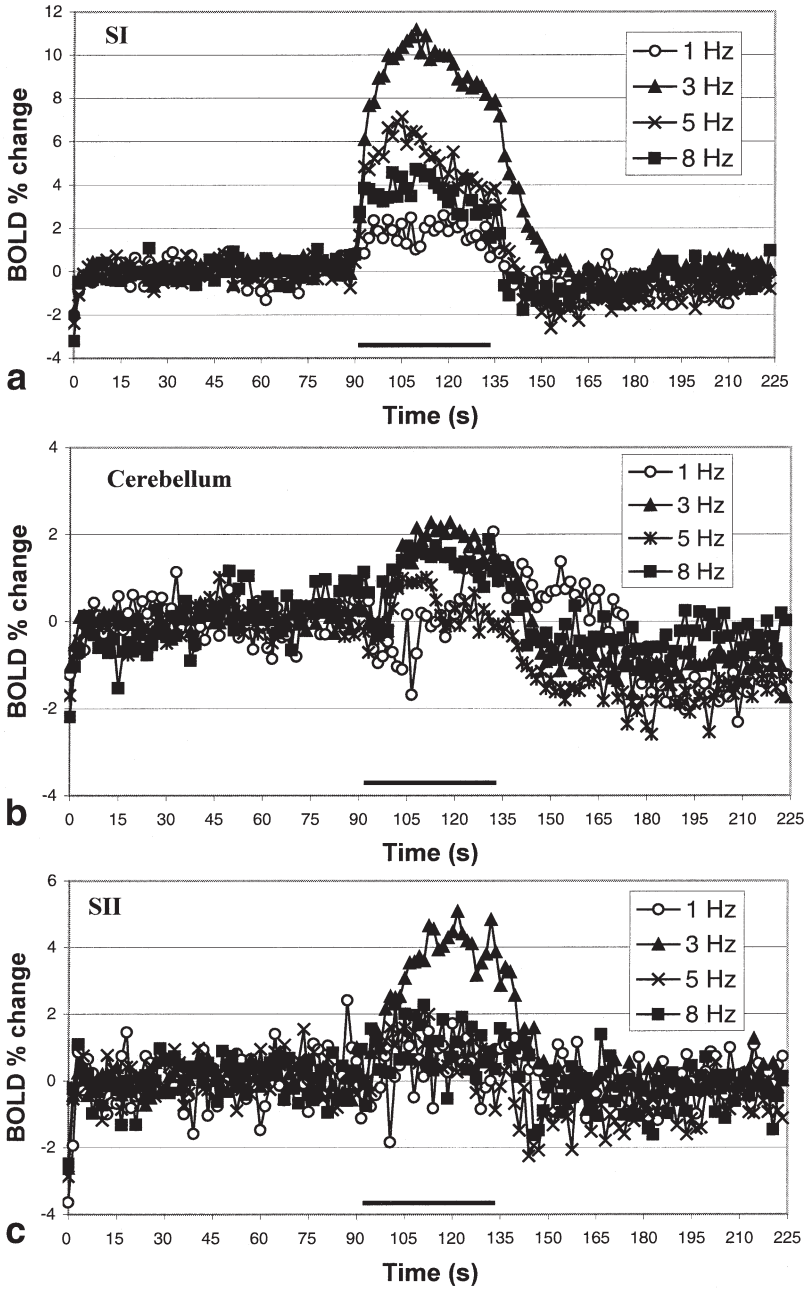

FIG. 10. Average time courses from SI (**a**), cerebellum (**b**), and SII (**c**) for stimulation frequencies of 1, 3, 5, and 8 Hz. The stimulation period is indicated by the black bar.

demonstrating maximal cortical activation at 3 Hz. We found that activation in the cerebellum and SII showed the same general frequency response as SI, with peak activation occurring at 3 Hz.

It is interesting to speculate on realizable goals for whole-brain fMRI of the rodent. Recently, a high-resolution fMRI study of SI during forepaw stimulation indicated a large heterogeneity in BOLD across the cortex at 200 μm resolution (14). In the same study, BOLD onset times as short as 600 ms could be detected. Thus, collecting whole-brain fMRI at 200 μm resolution with 500 ms temporal resolution would be a great advance. The increase of in-plane resolution from 300 to 200 μm can be readily achieved with slightly higher gradients, and this work is in progress. The reduction in acquisition time can also be readily accomplished, using parallel imaging techniques that are able to improve acquisition times 2–3-fold (32). In this study, the whole brain was imaged in 1–1.5 sec, so the acceleration provided by parallel imaging should improve this to ~500 ms. Further experiments will focus on determining the onset times of the activation in each area. This is particularly interesting because of the interaction between different regions of the brain. For example, if the cerebellum

activates earlier than the primary cortex, it may indicate that the primary source of the activation comes directly from the spinal cord, rather than from SI. However, the onset time differences may be dominated by the differing vasculature in each region, making it desirable to use whole-brain cerebral blood volume or perfusion fMRI to characterize the hemodynamic response.

Whole-brain fMRI of the rodent has the potential to shed light on many interesting neurological questions. It could be used to study changes that occur in the activated network during learning or plasticity after injury (24). Whole-brain functional imaging of the mouse is particularly interesting in light of the numerous disease models that are available. Many models show degeneration or reorganization of particular brain subsystems. fMRI provides a noninvasive way to examine the disrupted connections in these animals over the entire brain. This work demonstrates that whole-brain fMRI can be applied to the well-characterized rodent brain at 11.7 T, and establishes an important tool for the study of regional brain communication and plasticity.

ACKNOWLEDGMENTS

The authors thank Torri Wilson for animal preparation and physiology and Piotr Starewicz of Resonance Research, Inc., for the custom-built shim set.

REFERENCES

1. Hyde JS, Biswal BB, Jesmanowicz A. High-resolution fMRI using multislice partial k-space GR-EPI with cubic voxels. Magn Reson Med 2001;46:114–125.
2. Frank LR, Buxton RB, Wong EC. Estimation of respiration-induced noise fluctuations from undersampled multislice fMRI data. Magn Reson Med 2001;45:635–644.
3. Howseman AM, Grootoonk S, Porter DA, Ramdeen J, Holmes AP, Turner R. The effect of slice order and thickness on fMRI activation data using multislice echo-planar imaging. Neuroimage 1999;9:363–376.
4. Rombouts SA, Barkhof F, Hoogenraad FG, Sprenger M, Scheltens P. Within-subject reproducibility of visual activation patterns with functional magnetic resonance imaging using multislice echo planar imaging. Magn Reson Imag 1998;16:105–113.
5. Loenneker T, Hennel F, Hennig J. Multislice interleaved excitation cycles (MUSIC): an efficient gradient-echo technique for functional MRI. Magn Reson Med 1996;35:870–874.
6. Ogawa S, Lee TM, Kay AR, Tank DW. Brain magnetic resonance imaging with contrast dependent on blood oxygenation. Proc Natl Acad Sci USA 1990;87:9868–9872.
7. Williams DS, Detre JA, Leigh JS, Koretsky AP. Magnetic resonance imaging of perfusion using spin inversion of arterial water. Proc Natl Acad Sci USA 1992;89:212–216.
8. Mandeville JB, Marota JJ, Kosofsky BE, Keltner JR, Weissleder R, Rosen BR, Weisskoff RM. Dynamic functional imaging of relative cerebral blood volume during rat forepaw stimulation. Magn Reson Med 1998; 39:615–624.
9. Huang W, Plyka I, Li H, Eisenstein EM, Volkow ND, Springer CS, Jr. Magnetic resonance imaging (MRI) detection of the murine brain response to light: temporal differentiation and negative functional MRI changes. Proc Natl Acad Sci USA 1996;93:6037–6042.
10. Hyder F, Kida I, Behar KL, Kennan RP, Maciejewski PK, Rothman DL. Quantitative functional imaging of the brain: towards mapping neuronal activity by BOLD fMRI. NMR Biomed 2001;14:413–431.
11. Kida I, Kennan RP, Rothman DL, Behar KL, Hyder F. High-resolution CMR(O2) mapping in rat cortex: a multiparametric approach to calibration of BOLD image contrast at 7 Tesla. J Cereb Blood Flow Metab 2000;20:847–860.
12. Lee SP, Silva AC, Ugurbil K, Kim SG. Diffusion-weighted spin-echo fMRI at 9.4 T: microvascular/tissue contribution to BOLD signal changes. Magn Reson Med 1999;42:919–928.
13. Silva AC, Lee SP, Yang G, Iadecola C, Kim SG. Simultaneous blood oxygenation level-dependent and cerebral blood flow functional magnetic resonance imaging during forepaw stimulation in the rat. J Cereb Blood Flow Metab 1999;19:871–879.
14. Silva AC, Koretsky AP. Laminar specificity of functional MRI onset times during somatosensory stimulation in rat. Proc Natl Acad Sci USA 2002;99:15182–15187.
15. Ahrens ET, Dubowitz DJ. Peripheral somatosensory fMRI in mouse at 11.7 T. NMR Biomed 2001;14:318–324.
16. Bock C, Krep H, Brinker G, Hoehn-Berlage M. Brainmapping of alpha-chloralose anesthetized rats with T2*-weighted imaging: distinction between the representation of the forepaw and hindpaw in the somatosensory cortex. NMR Biomed 1998;11:115–119.
17. Lee SP, Silva AC, Kim SG. Comparison of diffusion-weighted high-resolution CBF and spin-echo BOLD fMRI at 9.4 T. Magn Reson Med 2002;47:736–741.
18. Ogawa S, Lee TM, Stepnoski R, Chen W, Zhu XH, Ugurbil K. An approach to probe some neural systems interaction by functional MRI at neural time scale down to milliseconds. Proc Natl Acad Sci USA 2000;97:11026–11031.
19. Spenger C, Josephson A, Klason T, Hoehn M, Schwindt W, Inguar M, Olson L. Functional MRI at 4.7 Tesla of the rat brain during electric stimulation of forepaw, hindpaw, or tail in single- and multislice experiments. Exp Neurol 2000;166:246–253.
20. Yang X, Hyder F, Shulman RG. Activation of single whisker barrel in rat brain localized by functional magnetic resonance imaging. Proc Natl Acad Sci USA 1996;93:475–478.
21. Kida I, Xu F, Shulman RG, Hyder F. Mapping at glomerular resolution: fMRI of rat olfactory bulb. Magn Reson Med 2002;48:570–576.
22. Xu F, Kida I, Hyder F, Shulman RG. Assessment and discrimination of odor stimuli in rat olfactory bulb by dynamic functional MRI. Proc Natl Acad Sci USA 2000;97:10601–10606.
23. Morton DW, Maravilla KR, Meno JR, Winn HR. Clinically relevant rat model for testing BOLD functional MR imaging techniques by using single-shot echo-planar imaging at 1.5 T. Radiology 2001;218:598–601.
24. Dijkhuizen RM, Ren J, Mandeville JB, et al. Functional magnetic resonance imaging of reorganization in rat brain after stroke. Proc Natl Acad Sci USA 2001;98:12766–12771.
25. Peeters RR, Verhoye M, Vos BP, Van Dyck D, Van der LA, De Schutter E. A patchy horizontal organization of the somatosensory activation of the rat cerebellum demonstrated by functional MRI. Eur J Neurosci 1999;11:2720–2730.
26. Paxinos G. The rat nervous system, 2nd ed. San Diego: Academic Press; 1995.
27. Paxinos G, Watson C. The rat brain in stereotaxic coordinates. San Diego: Academic Press; 1998.
28. Matsuura T, Kanno I. Quantitative and temporal relationship between local cerebral blood flow and neuronal activation induced by somatosensory stimulation in rats. Neurosci Res 2001;40:281–290.
29. Detre JA, Ances BM, Takahashi K, Greenberg JH. Signal averaged laser Doppler measurements of activation-flow coupling in the rat forepaw somatosensory cortex. Brain Res 1998;796:91–98.
30. Gyngell ML, Bock C, Schmitz B, Hoehn-Berlage M, Hossmann KA. Variation of functional MRI signal in response to frequency of somatosensory stimulation in alpha-chloralose anesthetized rats. Magn Reson Med 1996;36:13–15.
31. Brinker G, Bock C, Busch E, Krep H, Hossmann KA, Hoehn-Berlage M. Simultaneous recording of evoked potentials and T2*-weighted MR images during somatosensory stimulation of rat. Magn Reson Med 1999;41:469–473.
32. de Zwart JA, Ledden PJ, Kellman P, van Gelderen P, Duyn JH. Design of a SENSE-optimized high-sensitivity MRI receive coil for brain imaging. Magn Reson Med 2002;47:1218–1227.
33. de Zwart JA, van Gelderen P, Kellman P, Duyn JH. Application of sensitivity-encoded echo-planar imaging for blood oxygen level-dependent functional brain imaging. Magn Reson Med 2002;48:1011–1020.
34. Peeters RR, Tindemans I, De Schutter E, Van der LA. Comparing BOLD fMRI signal changes in the awake and anesthetized rat during electrical forepaw stimulation. Magn Reson Imag 2001;19:821–826.

35. Sicard K, Shen Q, Brevard ME, Sullivan R, Ferris CF, King JA, Duong TQ. Regional cerebral blood flow and BOLD responses in conscious and anesthetized rats under basal and hypercapnic conditions: implications for functional MRI studies. J Cereb Blood Flow Metab 2003;23:472–481.
36. Sachdev RN, Champney GC, Lee H, Price RR, Pickens DR III, Morgan VL, Stefansic JD, Melzer P, Ebner FF. Experimental model for functional magnetic resonance imaging of somatic sensory cortex in the unanesthetized rat. Neuroimage 2003;19:742–750.
37. Ogawa S, Menon RS, Kim SG, Ugurbil K. On the characteristics of functional magnetic resonance imaging of the brain. Annu Rev Biophys Biomol Struct 1998;27:447–474.
38. Silva AC, Lee SP, Iadecola C, Kim SG. Early temporal characteristics of cerebral blood flow and deoxyhemoglobin changes during somatosensory stimulation. J Cereb Blood Flow Metab 2000;20:201–206.
39. Ogawa S, Menon RS, Tank DW, Kim SG, Merkle H, Ellerman JM, Ugurbil K. Functional brain mapping by blood oxygenation level-dependent contrast magnetic resonance imaging. A comparison of signal characteristics with a biophysical model. Biophys J 1993;64: 803–812.
40. Weisskoff RM, Zuo CS, Boxerman JL, Rosen BR. Microscopic susceptibility variation and transverse relaxation: theory and experiment. Magn Reson Med 1994;31:601–610.